MEASUREMENT OF γ-RAY SPECTRA ACCOMPANYING RADIATIVE CAPTURE OF NUCLEONS

By J. S. Brzosko, E. Gierlik, A. Sołtan jr., Z. Szefliński and Z. Wilhelmi

"Stefan Pieńkowski" Institute of Experimental Physics, University of Warsaw*

(Received December 18, 1970)

Spectra of photons from the (n, γ) reaction have been measured for the ^{115}In, Sb, ^{127}I, ^{133}Cs, ^{159}Tb, ^{165}Ho, ^{181}Ta, ^{197}Au, Tl, and ^{238}U nuclei at neutron energies of about 400 keV. The dependence of the cross-sections for high energy γ-rays emission on neutron energy in the range 0.03 to 1.4 MeV was investigated for ^{115}In, ^{181}Ta, and ^{197}Au. Furthermore, γ-ray spectra for the (p, γ) reaction were measured and compared with those for the (n, γ) reaction.

The experimental results are compared with the results of calculation based on the compound nucleus model under the assumption that the probability of emission of γ-rays with energy of about 6 MeV is increased.

1. Introduction

The spectra of γ-rays accompanying radiative capture of neutrons were measured in a wide range of mass numbers both for thermal neutrons [1], [2], [3] and neutrons of energies exceeding 3 MeV [4], [5], [6].

In the works quoted it was found that there exists a bump in the high-energy part of the spectrum. This bump 1.5 MeV wide, occuring at γ-ray energies of about 6 MeV is particulary pronounced for nuclei with mass numbers close to $A = 60$, 130, and 200. Comparing spectra for various neutron energies it was found that the position of the bump does not change [7]. In order to explain the mechanism preferring so distinctly the emission of high energy γ-rays, Lane and Lynn [8] made an attempt to forward a theoretical description assuming a direct interaction. This approach does not, however, reproduce quantitatively the intensity of the high-energy γ-rays measured.

From the work of Wasson *et al.* [9] it follows that the emission from the compound nucleus is the basic mechanism involved in the emission of high energy γ-rays. However, for neutrons of higher energies the problem is far from clear. On the one hand the shape of the spectra [10], [11] and the absolute value of the cross-sections [11] are fairly well reproduced, assuming that the reaction proceeds through a compound nucleus. On the other hand, comparison of the γ-spectra measured for the (n, γ) reaction with those for the

* Address: Instytut Fizyki Doświadczalnej, Uniwersytet Warszawski, Warszawa, Hoża 69, Poland.

$(n, n'\gamma)$ [12] and $(d, p\gamma)$ [13] reactions suggests, according to the authors quoted, that the mechanism of high-energy γ-rays emission is connected with the disintegration of doorway states of the 2p−1h-type.

In this situation it seemed advisable to measure the cross-sections for high-energy γ-ray emission for various nuclei and different neutron energies, and to compare the γ-spectra accompanying neutron and proton capture.

2. *Measuring set up*

The method applied in this work was based on the measurement of γ-specta by means of a scintillation spectrometer with a NaI(Tl) crystal shielded from the neutrons by a layer of paraffin including lithium hydride and boron carbide (Fig. 1). The crystal was protected from the background by a 10 cm layer of lead.

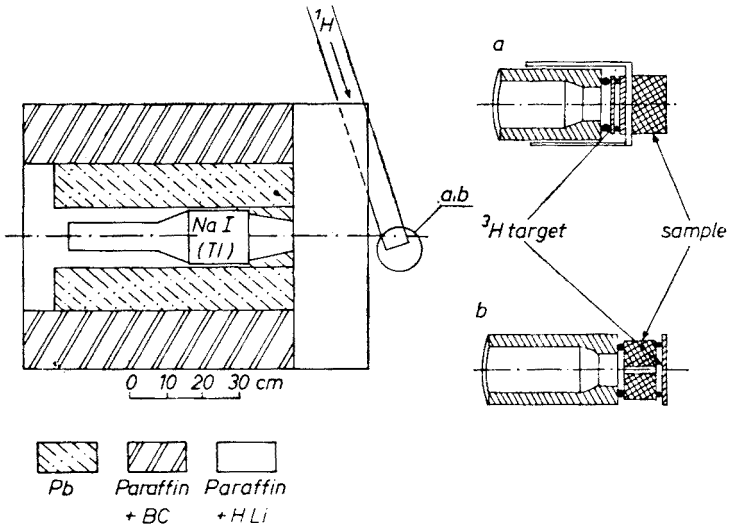

Fig. 1. Geometrical arrangement of the measuring system for the (n, γ) and (p, γ) reactions (see text)

The neutrons were obtained from the $^3H(p, n)^3He$ reaction, the protons being accelerated in the Van de Graaff accelerator in Warsaw. In the experiments considered neutron energies ranged from 40 keV ($E_p = 1330$ keV, $\theta \approx 140°$) to 1400 keV ($E_p = 2350$ keV, $\theta \approx 37°$), where θ is the angle between the directions of the protons and neutrons.

The main sources of the background were neutrons recorded by the NaI(Tl) crystal ($^{127}I(n, \gamma)$), the recorded γ-rays produced as a result of radiation capture of neutrons by the materials present in the measuring room, and the (n, γ) and (p, γ) reactions on nuclei of the backing of the tritium target. Therefore, apart from the shield system, a tritium target backing of special structure was applied [14]. This allowed for diminishing the backgrund so significantly that the principal contribution was due to the $^3H(p, \gamma)^4He$ reaction proceeding parallel to that constituting the source of neutrons.

The intensity of γ-radiation from the (n, γ) reaction was in general one to two times higher compared with that of the background. Since this ratio decreased with growing neutron energy, a proton pulsed beam ($\tau_{\text{pulse}} \approx 20$ μs) was additionally used for $E_n \geqslant 0.9$ MeV. The relevant methods is described in detail in Ref. [14]. The sole difference consisted in that in the latter work [14] a 4″×4″ NaI(Tl) crystal was used, whereas in the measurements described above the dimensions of the crystal were 3″×3″.

Since one of the components of the background was due to neutrons scattered elastically (from the sample studied) in the direction of the NaI(Tl) crystal, the background was measured so that the sample was substituted for a carbon cylinder of identical geometry and dimensions such that the differences in the scattering were less than 2% (the assessment being based on measurements in which use was made of a long counter). The absolute neutron flux was determined from the activity induced in the ^{197}Au$(n, \gamma)^{198}$Au reaction ($E\gamma = 412$ keV, $T_{1/2} = 2.703$ *d*). The relative variations in the neutron flux were observed by two independent methods. One consisted in measuring the intensity of neutrons moderated in the materials and walls of the target room using a proportional BF_3 counter. The second one consisted of recording by means of the scintillation counter the 20.3 MeV line due to the ^{3}H$(p, \gamma)^4$He reaction alongside the γ-spectrum studied. The latter method was also applied when use was made of the pulsed beam in the measurements.

The γ-spectrum was measured for the sample and carbon cylinder intermitently. Each series of measurements consisted of a dozen or so 10-minute irradiations, and for every neutron energy several such series of measurements were taken. Such a procedure was adopted because, as it was already mentioned, the effect and background were of comparable magnitudes, and from measurements of the variation of the background with time we have seen that the smooth fluctuations of about 20%, taking place, have a sufficiently long time of variation.

The procedure described allowed for good averaging of the contribution of the background to the spectrum measured, and the reproducibility of the results in each series of measurements convinced us that the averaging was adequate. The great simplicity of the method and comparatively short time of making use of the beam from the accelerator had to be compensated by lowered accuracy of the spectrum measured as compared with that which would be achieved if a pulsed ion source were used and a time-of-flight technique applied [5]. The main aim of our measurements was however, the determination of the cross-sections for γ-rays from the bump region, for which our method was much more suitable.

The spectra of pulses from the (n, γ) and (p, γ) reactions for the ^{115}In, ^{181}Ta, and ^{197}Au nuclei were also measured in the same geometry as shown in Fig. 1 using a scintillation spectrometer with a NaI(Tl) 4″×4″ crystal. Besides, γ-spectra were measured for Ag and ^{115}In from the (p, γ) reaction in the geometry shown in Fig. 2, and proton energy about 4 MeV using a NaI(Tl) 3″×3″ crystal.

The spectrum of pulses from the (p, γ) reaction for a given energy was obtained as a difference of two spectra for the energies $Ep + \Delta Ep$ and $Ep - \Delta Ep$ (where ΔEp is about 200 keV). The normalization of the spectra prior to deduction and the calculations of cross-sections were based on measuring the charge of protons on the target.

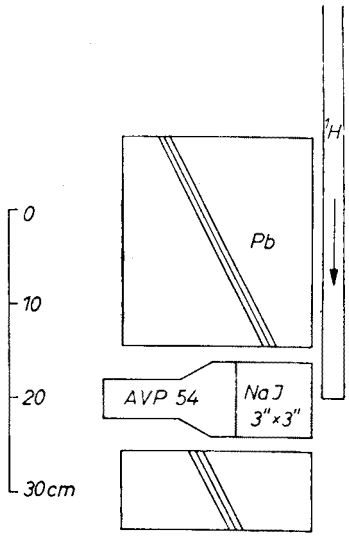

Fig. 2. Geometrical arrangement of the measuring system for the (p, γ) reactions

3. *Unfolding the spectra of pulses from the scintillation spectrometer*

An important point in the data handling was the conversion of pulse spectra measured to the spectra of γ-rays emitted as a result of radiation capture. To realize this objective an ITER programme [16] was developed which makes such a conversion possible. This programme based on the iterative method described by Mollenauer [17] solves the matrix equation

$$C_k = \sum_j R_{kj} N_j$$

where: C_k — is the number of pulses counted in the k-th analyser channel, N_j — the intensity of γ-radiation (of energy $E_\gamma = E_j$), R_{kj} — are the response matrix elements of the scintillation counter describing the probability of a γ-ray of energy E_j being recorded in the k-th channel.

As it follows from the matrix equation, the solutions of the problem requires the knowledge of the response matrix $||R||$ consisting of spectra of pulses corresponding to the recording of monoenergetic γ-rays. Such spectra have been described by us analytically in the form of a sum of expressions connected with the photoeffect, pair production, and Compton scattering. The photopeak, 1-st escape peak, and 2-nd escape peak were described by three Gaussian functions. The Compton effect was described by the Klein — Nishina equation diffused by the Gaussian function.

The particular components of the spectrum (and their parameters) were fitted by the least squares method to the five monoenergetic γ lines measured (2.76 MeV — ^{24}Na, 3.56 MeV — ^{9}Be$(p, \alpha\gamma)$, 4.43 MeV — PuBe-source, 6.13 MeV — ^{19}F$(p, \alpha\gamma)$, 7.48 MeV — ^{9}Be(p, γ)). Subsequently, the variation of parameters with energy was inter- and extrapolated making use of the values found for the above mentioned lines. Knowing the dependence of

the parameters describing the responce spectra on the energy of the primary γ-rays, a response function for every column of the $||R||$ matrix was developed in the range 2 to 10 MeV.

The errors of unfolding are due to the errors of the matrix used. According to our estimate the area under the γ-spectrum for $E_\gamma \geqslant 3.75$ MeV is determined with an accuracy up to 2% when the number of counts in the particular energy channels are burdened with errors up to 10%.

In Fig. 3 and 4 the shapes of pulse spectra recorded and of γ-rays are compared.

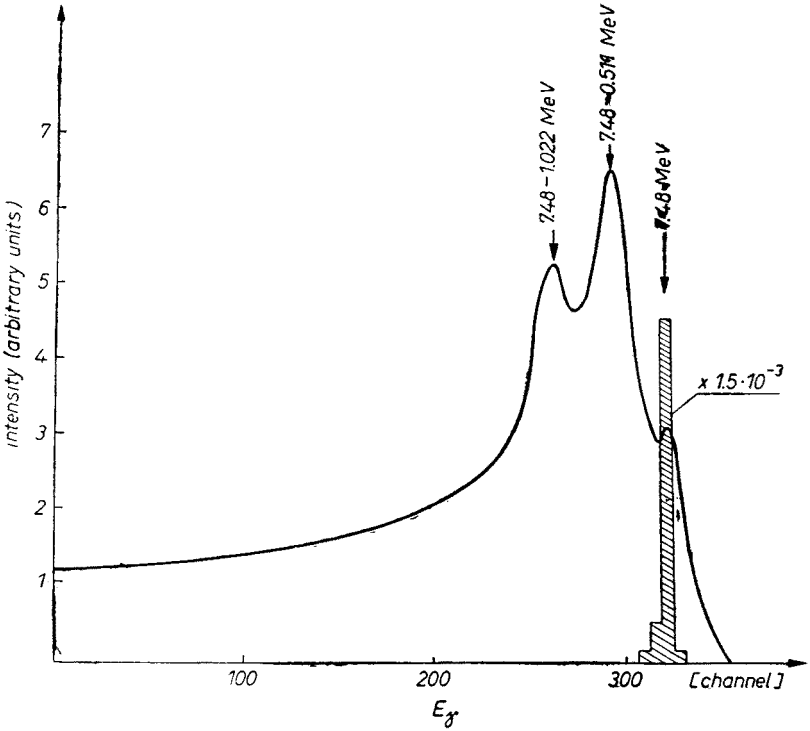

Fig. 3. Unfolding of the spectrum of 7.48 MeV monoline

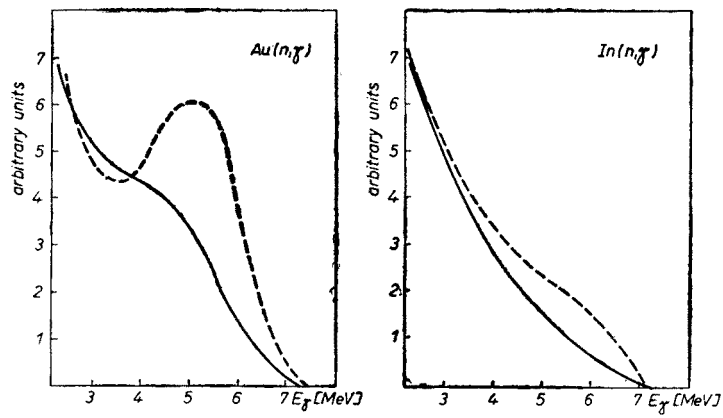

Fig. 4. Unfolding of the spectra; solid line — pulses spectrum, dashed line — γ-ray spectrum

The iterative method has been applied as it allows to interrupt the process of iteration at the moment the programme starts reproducing the statistical discontinuities of the pulse spectrum giving as a result nonphysical lines in the γ-spectrum.

4. Calculation of the cross-section for high-energy γ-ray emission

We determined the cross-sections $\frac{d\sigma_{n\gamma}}{dE_\gamma}$ and $\sigma_{n\gamma}(E_\gamma \geqslant 3.75\,\text{MeV})$ for high-energy γ-ray emission where $\sigma_{n\gamma}(E_\gamma \geqslant 3.75\,\text{MeV}) = \int_{3.75}^{E_n+B_n} \frac{d\sigma}{dE_\gamma}\, dE_\gamma$. The value $E_\gamma = 3.75\,\text{MeV}$ was selected, because above this γ-ray energy we observe the anomalous bump which was the object of our study.

The cross-sections were calculated from the relation:

$$\frac{\sigma_{n\gamma}(E_\gamma \geqslant 3.75\,\text{MeV})}{\sigma_{n\gamma}^{\text{Au}}} = \delta \frac{N_\gamma}{n_X \alpha_X} \left(\frac{A_0}{n_{\text{Au}} \alpha_{\text{Au}}}\right)^{-1}$$

where: $\sigma_{n\gamma}^{\text{Au}}$ — cross-section for $^{197}\text{Au}(n, \gamma)^{198}\text{Au}$ reaction; N_γ — the number of pulse recorded in the channels corresponding to $E_\gamma \geqslant 3.75\,\text{MeV}$; δ — the factor converting the number N_γ of pulses recorded to that of γ-rays emitted by the sample in the round solid angle (for $E_\gamma \geqslant 3.75\,\text{MeV}$). This value was calculated making use of the ITER programme; n — a magnitude proportional (with coefficient α) to the neutron flux passing through the sample — counts of the BF_3 counter, or number of γ-rays of $E_\gamma = 20.3\,\text{MeV}$ ($^3\text{H}(p, \gamma)^4\text{He}$). The neutron flux passing through the Au sample is $\Phi_{\text{Au}} = \alpha_{\text{Au}} \cdot n_{\text{Au}}$, and that passing through the sample X is $\Phi_X = \alpha_X \cdot n_X$; A — the activity of the Au sample measured, used for the determination of the absolute neutron flux. The absolute activity A_0 was found from the relation $A_0 = \frac{A}{\varkappa}$. The activity was measured by observing the disappearance of the 412 keV line ($T_{1/2} = 2.703$ d) by means of a NaI(Tl) $2'' \times 2''$ scintillation counter. The value of $\varkappa$ was calculated using the KAPPA programme [18].

The KAPPA programme was applied for simulating by a computer the experiment of sample activation. It allowed to calculate the activity distribution on the basis of known angle distributions of the neutron flux [19], the dependence of $\sigma_{n\gamma}$ on the neutron energy, and the irradiation geometry. Subsequently, making use of the activity distribution obtained the KAPPA programme predicted the measured disintegration rate A taking account of self-absorption in the sample, geometry of the measuring set up and efficiency of the counter. The value of $\varkappa$ obtained satisfied the relation $A_0\varkappa = A$. Taking account of the uncertainty of the distributions used, determination of the geometry, computational approximations, *etc.*, the probable error of the calculated magnitude $\varkappa$ was estimated at about 2%. This result was confirmed by additional control measurement. The programme described also estimated the average energy and the energy diffusion of neutrons incident on the sample. The typical values of $\varkappa$ were 7.10^{-3}. Alongside the values of $\varkappa$ the α values were calculated providing for the differences in the geometry of irradiation of the Au sample

(used to get the absolute neutron flux) and of the sample X for which the γ-spectrum was studied.

Since in the procedure adopted a significant part was played by the good knowledge of $\sigma_{n\gamma}$, the neutron flux was determined in all cases on the basis of the $^{197}Au(n, \gamma)^{198}Au$ reaction.

When studying the (p, γ) reaction the cross-section was found from the relation

$$\sigma_{p\gamma}(E_\gamma \geqslant 3.75 \text{ MeV}) = \frac{\delta N_\gamma}{\Phi \nu}$$

where: $\delta \cdot N_\gamma$ is the number of γ-rays emitted in the (p, γ) reaction; Φ — the number of protons as determined by the integrator, which were cause of recording N_γ pulses by the scintillation spectrometer; ν — number of nuclei per sq cm of the irradiated sample whose thickness corresponds to the energy loss of the protons by $2 \cdot \Delta E_p$.

5. *Results*

The measured γ-spectra are presented in Fig. 5. The spectra obtained by us and the values measured (Fig. 6) support the conclusion forwarded by Bergqvist [4] that the intensity of the bump increases for mass numbers of about 130 and 200.

In Fig. 7 $\frac{\sigma_{n\gamma}(E_\gamma \geqslant 3.75\text{MeV})}{\sigma_{n\gamma}}$ is presented as a function of the energy of neutrons initiating the reaction for ^{115}In, ^{181}Ta, and ^{197}Au. The values measured were compared with those calculated from the compound nucleus model (Figs 5 and 7). These calculations were performed similarily as in Ref. [11], assuming that the probability of γ-emission is proportional to the cross-section for γ-absorption. It was assumed that in the cross-section for γ-absorption alongside the giant resonance $E1$ its echo is found in the form of a small peak lying, depending on the mass number of the nucleus, at the γ-ray energy of about 5.5 — 8 MeV.

In Fig. 8 the spectra of pulses from the (n, γ) and (p, γ) reactions are compared (the spectra were normalized at 3 MeV). It is striking that both spectra coincide when ^{197}Au (nucleus for which a bump is observed) is used as a target. For ^{115}In and ^{181}Ta nuclei the spectra obtained for the (p, γ) reaction are in their high-energy part definitely more pronounced.

In Fig. 9 γ-ray spectra for the (p, γ) reaction on Ag, In, Ta and Au are compared with calculations. The theoretical predictions were achieved on the base of the compound nucleus model with statistical de-excitation. The probability of a photon emission was used in the following form:

$$\left(\frac{\Gamma}{D}\right) \propto E_\gamma \sigma_a(E_\gamma) \varrho(U - E_\gamma)$$

where: ϱ — density of final nucleus levels; E_γ — energy of an emitted photon; U — excitation energy of the nucleus; σ_a — photon absorption cross-section.

The absorption cross-section σ_a was presented in analytical form as a sum of two terms. The first term describes the giant resonance $E1$, the second one — the echo resonance [11].

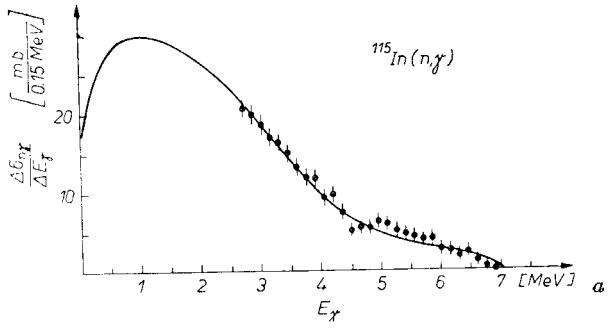
$^{115}In(n,\gamma)$
$\frac{\Delta\sigma_{n\gamma}}{\Delta E_\gamma}$ $\left[\frac{mb}{0.15\,MeV}\right]$
20
10
1 2 3 4 5 6 7 [MeV]
E_γ

a

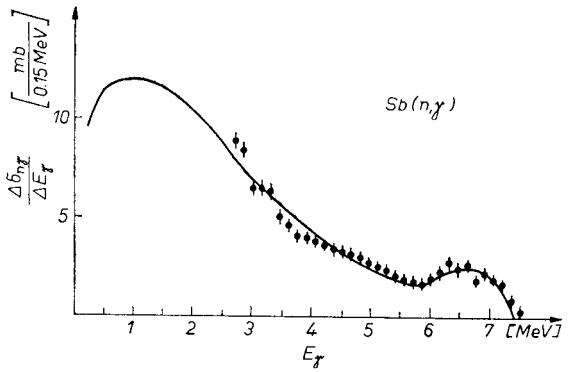
$Sb(n,\gamma)$
$\frac{\Delta\sigma_{n\gamma}}{\Delta E_\gamma}$ $\left[\frac{mb}{0.15\,MeV}\right]$
10
5
1 2 3 4 5 6 7 [MeV]
E_γ

b

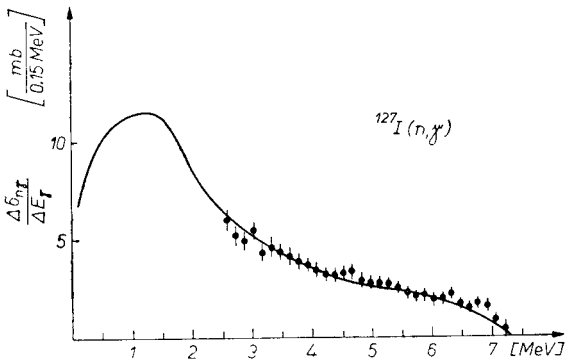
$^{127}I(n,\gamma)$
$\frac{\Delta\sigma_{n\gamma}}{\Delta E_\gamma}$ $\left[\frac{mb}{0.15\,MeV}\right]$
10
5
1 2 3 4 5 6 7 [MeV]

c

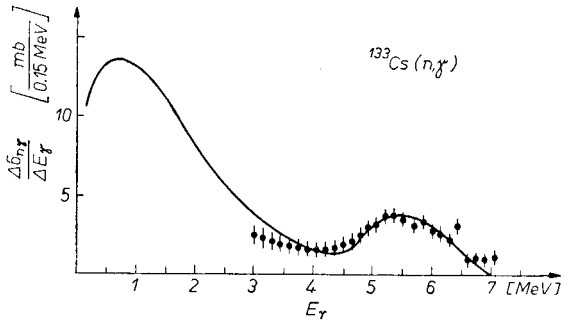
$^{133}Cs(n,\gamma)$
$\frac{\Delta\sigma_{n\gamma}}{\Delta E_\gamma}$ $\left[\frac{mb}{0.15\,MeV}\right]$
10
5
1 2 3 4 5 6 7 [MeV]
E_γ

d

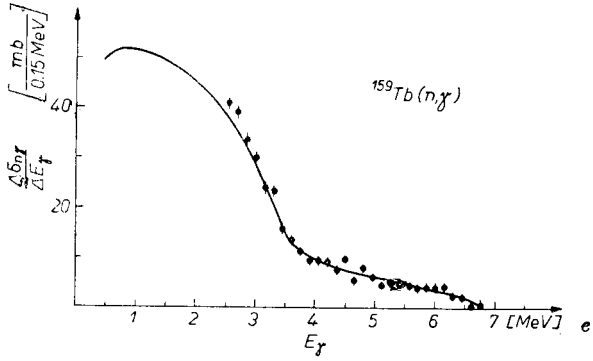
159Tb (n,γ)
40
20
1 2 3 4 5 6 7 [MeV]
Eγ

e

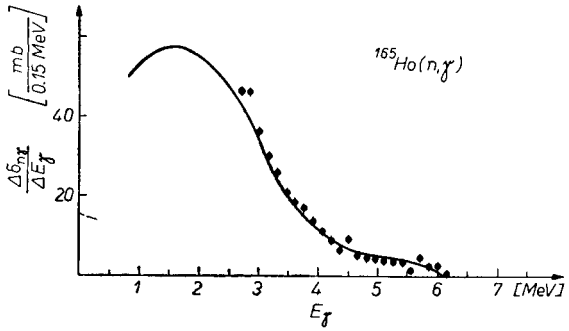
165Ho(n,γ)
40
20
1 2 3 4 5 6 7 [MeV]
Eγ

f

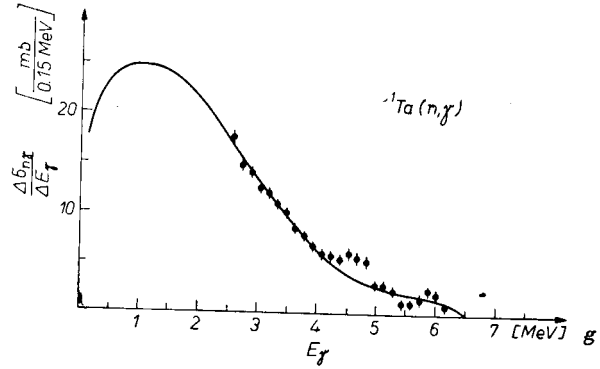
181Ta (n,γ)
20
10
1 2 3 4 5 6 7 [MeV]
Eγ

g

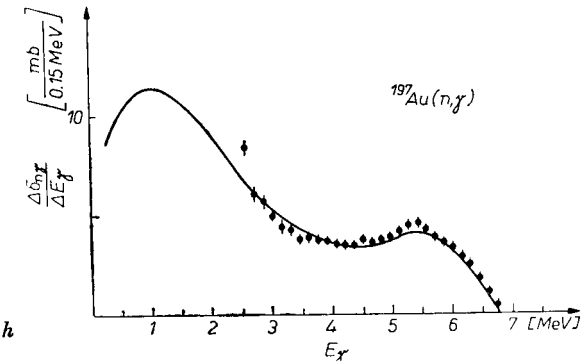
197Au(n,γ)
10
1 2 3 4 5 6 7 [MeV]
Eγ

h

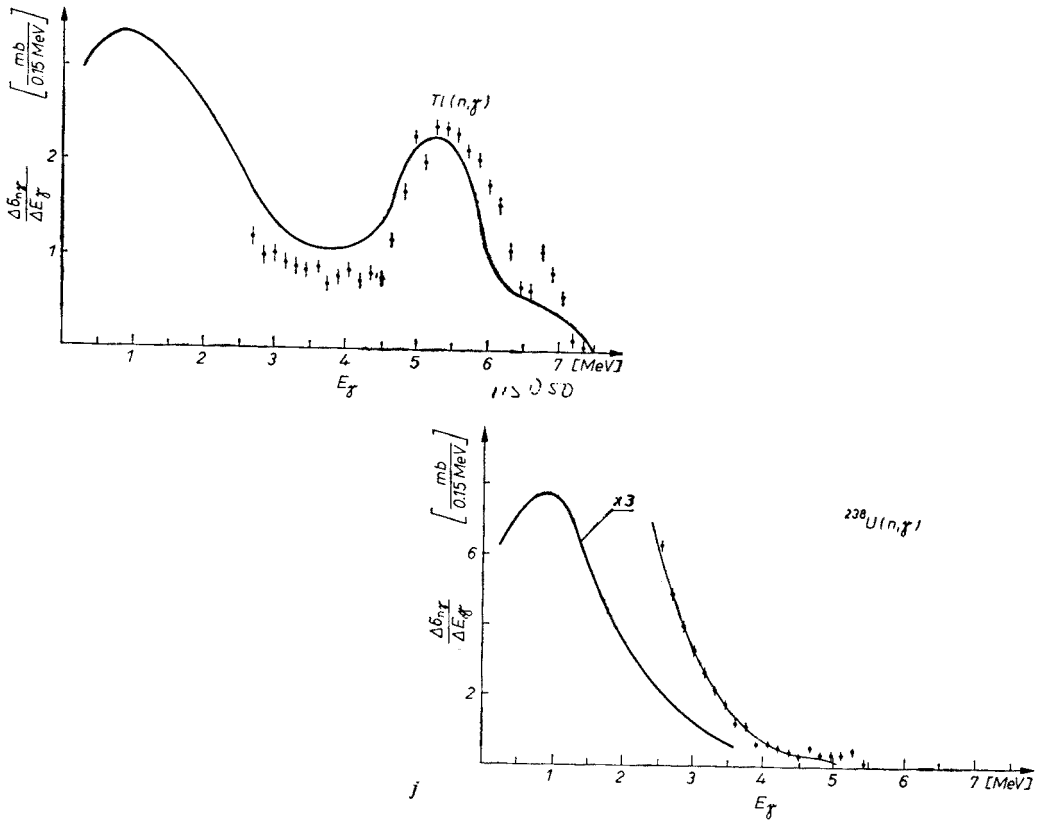

Fig. 5*a–j*. γ-ray spectrum for the ^{115}In(n, γ) reaction; solid line — calculated gamma spectrum taking account of the echo-resonance. Neutron energy $E_n \approx 400$ keV

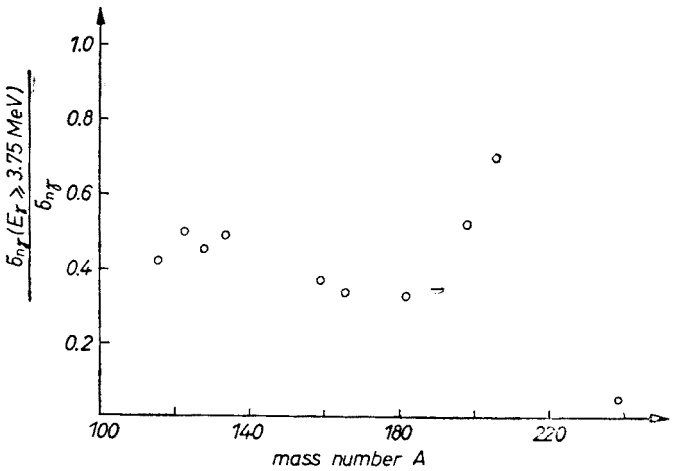

Fig. 6. $\frac{\sigma_{n\gamma}(E_\gamma \geqslant 3.75\ \text{MeV})}{\sigma_{n\gamma}}$ *versus* mass number A

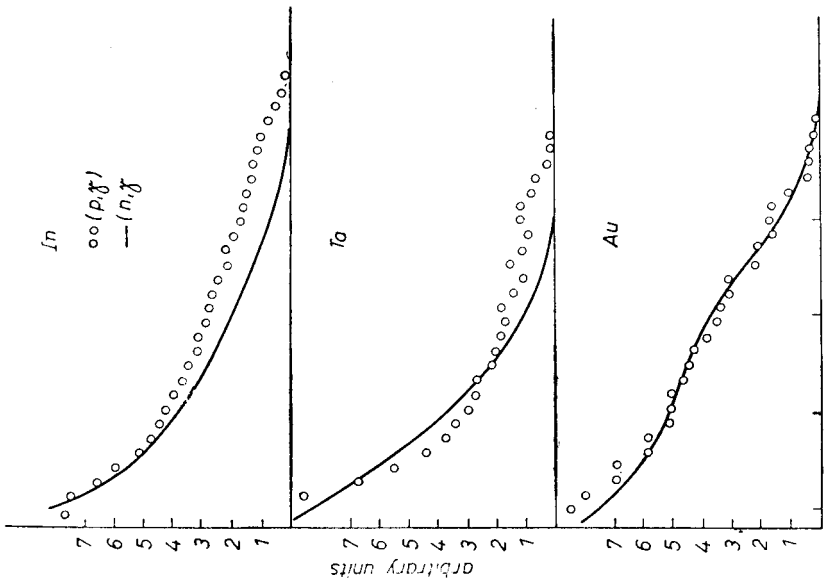

Fig. 8

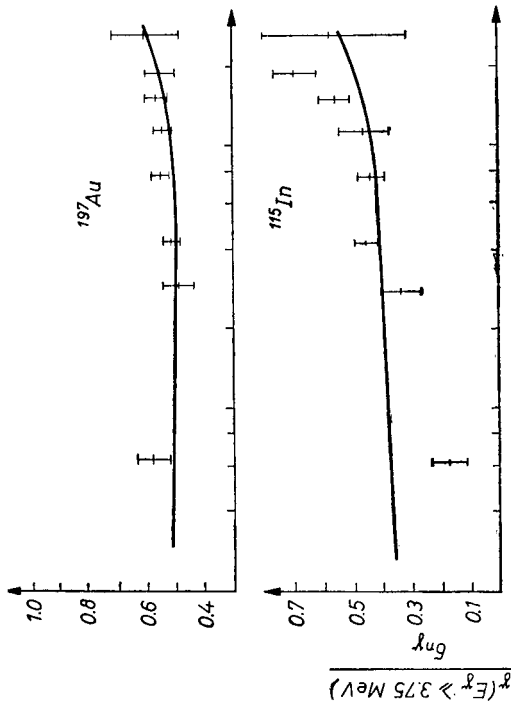

Fig. 7

Fig. 7. $\frac{\sigma_{n\gamma}(E_\gamma \geqslant 3.75\ \mathrm{MeV})}{\sigma_{n\gamma}}$ *versus* neutron energy E_n

Fig. 8. Comparison of the pulses spectra from the (n, γ) and (p, γ) reactions (NaI 4″×4″)

The mentioned form is the following:

$$\sigma_a = 0.0133 \frac{NZ}{A} E_\gamma \left\{ \frac{\Gamma_1 \exp\left[d(E_\gamma - E_{R_1})\right]}{E_{R_1}\left[(E_\gamma - E_{R_1})^2 + \Gamma_2^2/4\right]} + b \frac{\Gamma_2 \exp\left[d(E_\gamma - E_{R2})\right]}{E_{R2}\left[(E_\gamma - E_{R2})^2 + \Gamma_2^2/4\right]} \right\}$$

where: A, N, Z — mass number, neutron number, and proton number of target nucleus respectively, Γ_1, E_{R1} — width and energy of giant resonance respectively, Γ_2, E_{R2} — the respective values corresponding to the echo resonance, d — shape parameter of the resonances, b — parameter determining the relative contribution of the echo resonance with respect to the giant resonance.

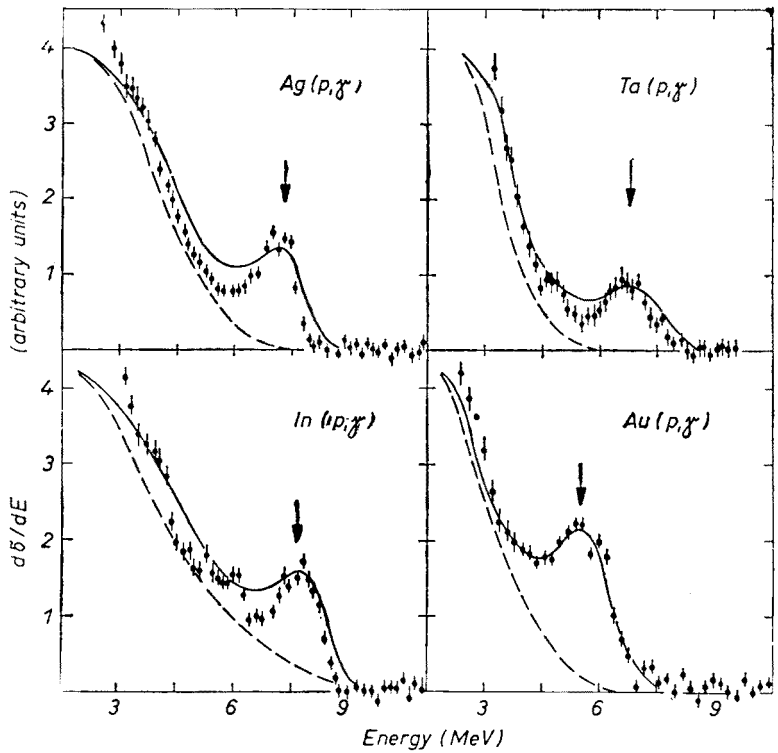

Fig. 9. γ-ray spectrum from the (p, γ) reactions; solid line — calculated gamma spectrum taking account of the echo resonance, dashed line — calculation without use of echo resonance. Proton energy $E_p \approx 4$ MeV. The cross-sections $\frac{d\sigma}{dE}$ for E_γ above bump up to an energy equal excitation energy are very small but different from zero

The absence of the bump in the high-energy part of the spectrum for the $^{115}\mathrm{In}(n, \gamma)$ reaction may be explained by energy conditions. The echo-resonance occurs in In at $E_\gamma \approx 8$ MeV, and hence at E_n up to 1.3 MeV ($B_n = 6.6$ MeV) it is initiated but slightly.

The results considered here are summarized in Table I, but the parameters of the echo-resonance, used in theoretical calculations, are listed in Table II.

TABLE I

Measured and calculated cross-section for γ-rays emission in the (n, γ) and (p, γ) reactions

Reaction	Measured values			Calculated values	
	$\sigma_{N,\gamma}$ ($E_\gamma \geqslant 3.75$ MeV) [mb]	$\sigma_{n,\gamma}$[mb]	$\sigma_{n,\gamma}$ ($E_n \geqslant 3.75$MeV)/ $\sigma_{n,\gamma}$	Compound nucleus model [mb]	Direct interaction model [μb]
^{115}In (n, γ)	108±7	250	0.43 ±0.05	127	0.026
Sb (n, γ)	65±5	130	0.50 ±0.05	74	0.1
^{127}I (n, γ)	67±5	150	0.44 ∓0.03	67	0.17
^{133}Cs (n, γ)	60±15	150	0.40 ±0.08	65	230
^{159}Tb (n, γ)	125±9	350	0.37 ±0.05	145	—
^{165}Ho (n, γ)	102±7	300	0.37 ±0.05	107	0.055
^{181}Ta (n, γ)	68±5	205	0.34 ±0.05	55	0.08
^{197}Au (n, γ)	104±8	190	0.53 ±0.03	108	0.021
Tl (n, γ)	28±3	40	0.70 ±0.07	32	0.1
^{238}U (n, γ)	6.3±0.5	127	0.050±0.005	7.1	—
Ag (p, γ)	0.50±0.10	—	—	—	—
^{115}In (p, γ)	0.16±0.03	—	—	—	—
^{181}Ta (p, γ)	0.035±0.015	—	—	—	—
^{197}Au (p, γ)	0.035±0.015	—	—	—	—

TABLE II

Parameters used in theoretical calculations. Optical model parameters were obtained as: $U_N = 52.5-0.6E$ $W_N = 2.5+0.3E$; $U_{LS} = 10.0-0.15E$; $W_{LS} = 0$ MeV

Nucleus	E_{R_2} [MeV]	Γ_2 [MeV]	b	V_N [MeV]	V_{LS} [MeV]
Ag	7	1.5	0.008		
^{115}In	8	2	0.03	−47.8	−16.8
^{121}Sb	6.8	1.5	0.003	−47.5	−16.5
^{127}I	6.5	1.5	0.005	−47.3	−16.2
^{133}Cs	6	1.4	0.002	−47.0	−16.0
^{159}Tb	6.2	1.8	0.007	—	—
^{165}Ho	6.8	1.5	0.002	−43.0	−14.8
^{181}Ta	7	1.5	0.002	−43.2	−15.2
^{197}Au	5.5	1.0	0.05	−43.6	−17.1
Hg	5.5	1.0	0.01	—	—
Tl	5.2	1.0	0.001	−46.1	−15.1
Pb	6.2	1.3	0.008	—	—
^{209}Bi	6.0	2	—	—	—
^{238}U	6.5	1.7	0.04	—	—

V_N — depth of Saxon-Woods potential.
V_{LS} — depth of spin-orbit potential.

6. *Recapitulation*

As it is seen from the presented material, based on the compound nucleus model taking account of the echo-resonance, it is possible to reproduced the experimental data gathered for the (n, γ) and (p, γ), reactions. The quantitative and qualitative agreement obtained suggests that the approach adopted is adequate.

Important information is obtained from the comparison of γ-spectra for the (n, γ) and (p, γ) reactions. These spectra, considering the difference in the initiation energies for which they were observed, show similar tendencies as regards the amplification of the γ transitions revealed for E_γ of about 6–8 MeV. This amplification is related to the resonance in the excitation function for absorption of γ-rays of the same energy.

The autors wish to express their thanks to the Management of the Joint Institute of Nuclear Research for allowing them to conduct part of irradiation experiments on the Van de Graaff accelerator at the Laboratory of Nuclear Physics in Dubna.

REFERENCES

[1] G. A. Bartholomew, *Amer. Rev. Nuclear Science*, **11**, 259 (1961).
[2] G. A. Bartholomew, A. Doveika, K. M. Eastwood, S. Morano, L. V. Groshev, A. M. Demidov, V. I. Pelekhov, L. Sokolovskii, *Nuclear Data*, **A3** (1967) Nos 4, 5 and 6.
[3] L. V. Groshev, A. M. Demidov, V. I. Pelekhov, L. Sokolovskii, G. A. Bartholomew, A. Doveika, K. M. Eastwood, S. Morano, *Nuclear Data*, **A5** (1968) Nos 1 and 2.
[4] I. Bergqvist, N. Starfelt, *Nuclear Phys.*, **22**, 513 (1961).
[5] I. Bergqvist, N. Starfelt, *Nuclear Phys.*, **39**, 353 (1962).
[6] B. Lundberg, N. Starfelt, *Nuclear Phys.*, **67**, 321 (1965).
[7] I. Bergqvist, N. Starfelt, *Nuclear Phys.*, **39**, 529 (1962).
[8] A. M. Lane, J. E. Lynn, *Nuclear Phys.*, **17**, 563, 586 (1960).
[9] O. A. Wasson, J. E. Draper, *Nuclear Phys.*, **73**, 499 (1965).
[10] N. Starfelt, *Nuclear Phys.*, **53**, 397 (1964).
[11] J. S. Brzosko, E. Gierlik, A. Sołtan jr, Z. Wilhelmi, *Canad. J. Phys.*, **47**, 2849 (1969).
[12] I. Bergqvist, B. Lundberg, L. Nilsson, N. Starfelt, *Nuclear Phys.*, **80**, 198 (1966).
[13] G. A. Bartholomew, E. D. Earle, A. J. Ferguson, I. Bergqvist, *Canad. J. Phys.*, **48**, 487 (1970).
[14] J. S. Brzosko, E. Gierlik, A. Sołtan jr, Z. Wilhelmi, *Report INR* 1224/I/PL (1970).
[15] I. Bergqvist, B. Lundberg, L. Nilsson, N. Starfelt, *Nuclear Phys.*, **A120**, 161 (1968).
[16] Z. Szefliński, University of Warsaw, Inst. Exp. Phys., programme ITER.
[17] J. F. Mollenauer, *Report UCRL* — 9748 (1961).
[18] A. Sołtan jr, University of Warsaw, Inst. Exp. Phys., programme KAPPA.
[19] N. Jarmie, J. D. Seagrave, *Report LA* — 2014 (1957).